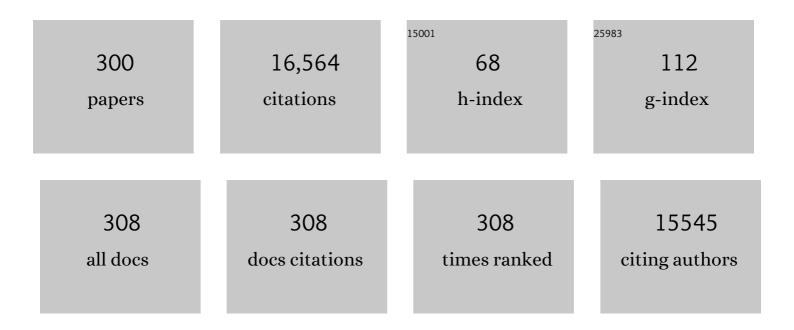
List of Publications by Year in descending order

Source: https://exaly.com/author-pdf/2596027/publications.pdf Version: 2024-02-01



#	Article	IF	CITATIONS
1	Disulfide Bonds Play a Critical Role in the Structure and Function of the Receptor-binding Domain of the SARS-CoV-2 Spike Antigen. Journal of Molecular Biology, 2022, 434, 167357.	2.0	43
2	Mercury Lα1 High Energy Resolution Fluorescence Detected X-ray Absorption Spectroscopy: A Versatile Speciation Probe for Mercury. Inorganic Chemistry, 2022, 61, 5201-5214.	1.9	7
3	Molecular Fates of Organometallic Mercury in Human Brain. ACS Chemical Neuroscience, 2022, 13, 1756-1768.	1.7	12
4	Synthesis and structural characterization of copper–cuprizone complexes. Dalton Transactions, 2022, 51, 10361-10376.	1.6	3
5	Hg(II) Binding to Thymine Bases in DNA. Inorganic Chemistry, 2021, 60, 7442-7452.	1.9	7
6	Geometry of Pentaphenylantimony in Solution: Support for a Trigonal Bipyramidal Assignment from X-ray Absorption Spectroscopy and Vibrational Spectroscopic Data. Inorganic Chemistry, 2021, 60, 8566-8574.	1.9	4
7	High Energy Resolution Fluorescence Detected X-ray Absorption Spectroscopy: An Analytical Method for Selenium Speciation. Analytical Chemistry, 2021, 93, 9235-9243.	3.2	14
8	Sulfur Kβ X-ray emission spectroscopy: comparison with sulfur K-edge X-ray absorption spectroscopy for speciation of organosulfur compounds. Physical Chemistry Chemical Physics, 2021, 23, 4500-4508.	1.3	18
9	Oxygen K-edge X-ray absorption spectra of liquids with minimization of window contamination. Journal of Synchrotron Radiation, 2021, 28, 1845-1849.	1.0	2
10	Abridged spectral matrix inversion: parametric fitting of X-ray fluorescence spectra following integrative data reduction. Journal of Synchrotron Radiation, 2021, 28, 1881-1890.	1.0	0
11	The Unexpected Role of Se ^{VI} Species in Epoxidations with Benzeneseleninic Acid and Hydrogen Peroxide. Angewandte Chemie - International Edition, 2020, 59, 4283-4287.	7.2	22
12	PIN FORMED 2 Modulates the Transport of Arsenite in Arabidopsis thaliana. Plant Communications, 2020, 1, 100009.	3.6	17
13	Human red blood cell uptake and sequestration of arsenite and selenite: Evidence of seleno-bis(S-glutathionyl) arsinium ion formation in human cells. Biochemical Pharmacology, 2020, 180, 114141.	2.0	7
14	Structural Characterization of the Solution Chemistry of Zirconium(IV) Desferrioxamine: A Coordination Sphere Completed by Hydroxides. Inorganic Chemistry, 2020, 59, 17443-17452.	1.9	13
15	PBT2 acts through a different mechanism of action than other 8-hydroxyquinolines: an X-ray fluorescence imaging study. Metallomics, 2020, 12, 1979-1994.	1.0	13
16	Copper(II) Binding to PBT2 Differs from That of Other 8-Hydroxyquinoline Chelators: Implications for the Treatment of Neurodegenerative Protein Misfolding Diseases. Inorganic Chemistry, 2020, 59, 17519-17534.	1.9	15
17	X-ray absorption spectroscopy of organic sulfoxides. RSC Advances, 2020, 10, 26229-26238.	1.7	5
18	Solution Chemistry of Copper(II) Binding to Substituted 8-Hydroxyquinolines. Inorganic Chemistry, 2020, 59, 13858-13874.	1.9	6

#	Article	IF	CITATIONS
19	Sample preparation with sucrose cryoprotection dramatically alters Zn distribution in the rodent hippocampus, as revealed by elemental mapping. Journal of Analytical Atomic Spectrometry, 2020, 35, 2498-2508.	1.6	19
20	Reply to Comments on "Rethinking the Minamata Tragedy: What Mercury Species Was Really Responsible?― Environmental Science & Technology, 2020, 54, 8484-8485.	4.6	3
21	Studies of selenium and arsenic mutual protection in human HepG2 cells. Chemico-Biological Interactions, 2020, 327, 109162.	1.7	7
22	Reply to Comments on "Rethinking the Minamata Tragedy: What Mercury Species Was Really Responsible?― Environmental Science & Technology, 2020, 54, 8488-8490.	4.6	5
23	Direct Observation of Methylmercury and Auranofin Binding to Selenocysteine in Thioredoxin Reductase. Inorganic Chemistry, 2020, 59, 2711-2718.	1.9	43
24	The Unexpected Role of Se VI Species in Epoxidations with Benzeneseleninic Acid and Hydrogen Peroxide. Angewandte Chemie, 2020, 132, 4313-4317.	1.6	1
25	Rethinking the Minamata Tragedy: What Mercury Species Was Really Responsible?. Environmental Science & Technology, 2020, 54, 2726-2733.	4.6	40
26	Prolonged Blood-Brain Barrier Injury Occurs After Experimental Intracerebral Hemorrhage and Is Not Acutely Associated with Additional Bleeding. Translational Stroke Research, 2019, 10, 287-297.	2.3	38
27	Bimodal Nickel-Binding Site on <i>Escherichia coli</i> [NiFe]-Hydrogenase Metallochaperone HypA. Inorganic Chemistry, 2019, 58, 13604-13618.	1.9	8
28	Elemental characterisation of the pyramidal neuron layer within the rat and mouse hippocampus. Metallomics, 2019, 11, 151-165.	1.0	19
29	Disruption of selenium transport and function is a major contributor to mercury toxicity in zebrafish larvae. Metallomics, 2019, 11, 621-631.	1.0	19
30	Visualizing sulfur with X-rays: From molecules to tissues. Phosphorus, Sulfur and Silicon and the Related Elements, 2019, 194, 618-623.	0.8	3
31	X-ray Absorption Spectroscopy Investigations of Copper(II) Coordination in the Human Amyloid β Peptide. Inorganic Chemistry, 2019, 58, 6294-6311.	1.9	30
32	Sulfur K-Edge X-ray Absorption Spectroscopy of Aryl and Aryl–Alkyl Sulfides. Journal of Physical Chemistry A, 2019, 123, 2861-2866.	1.1	4
33	The effects of dietary selenomethionine on tissue-specific accumulation and toxicity of dietary arsenite in rainbow trout (<i>Oncorhynchus mykiss</i>) during chronic exposure. Metallomics, 2019, 11, 643-655.	1.0	13
34	Wide field imaging energy dispersive X-ray absorption spectroscopy. Scientific Reports, 2019, 9, 17734.	1.6	9
35	Revealing the Penumbra through Imaging Elemental Markers of Cellular Metabolism in an Ischemic Stroke Model. ACS Chemical Neuroscience, 2018, 9, 886-893.	1.7	19
36	Cryoprotectants Severely Exacerbate X-ray-Induced Photoreduction. Journal of Physical Chemistry Letters, 2018, 9, 540-544.	2.1	13

#	Article	IF	CITATIONS
37	X-ray spectroscopy and imaging of selenium in living systems. Biochimica Et Biophysica Acta - General Subjects, 2018, 1862, 2383-2392.	1.1	16
38	A comparison of parametric and integrative approaches for X-ray fluorescence analysis appliedÂto a Stroke model. Journal of Synchrotron Radiation, 2018, 25, 1780-1789.	1.0	11
39	Ajothiolanes: 3,4-Dimethylthiolane Natural Products from Garlic (<i>Allium sativum</i>). Journal of Agricultural and Food Chemistry, 2018, 66, 10193-10204.	2.4	19
40	A Photochemically Generated Selenyl Free Radical Observed by High Energy Resolution Fluorescence Detected X-ray Absorption Spectroscopy. Inorganic Chemistry, 2018, 57, 10867-10872.	1.9	14
41	X-ray-Induced Photoreduction of Hg(II) in Aqueous Frozen Solution Yields Nearly Monatomic Hg(0). Inorganic Chemistry, 2018, 57, 8205-8210.	1.9	3
42	X-ray Absorption Spectroscopy of Metals in Biology. , 2018, , 1-7.		0
43	X-ray Fluorescence Imaging: Elemental and Chemical Speciation Mapping of Biological Systems. , 2018, , 1-6.		0
44	Superior spatial resolution in confocal X-ray techniques using collimating channel array optics: elemental mapping and speciation in archaeological human bone. Journal of Analytical Atomic Spectrometry, 2017, 32, 527-537.	1.6	21
45	Mononuclear Sulfido-Tungsten(V) Complexes: Completing the Tp*MEXY (M = Mo, W; E = O, S) Series. Inorganic Chemistry, 2017, 56, 5189-5202.	1.9	6
46	The active site structure and catalytic mechanism of arsenite oxidase. Scientific Reports, 2017, 7, 1757.	1.6	25
47	Binding of Copper and Cisplatin to Atox1 Is Mediated by Glutathione through the Formation of Metal–Sulfur Clusters. Biochemistry, 2017, 56, 3129-3141.	1.2	27
48	Optimization of overexpression of a chaperone protein of steroid C25 dehydrogenase for biochemical and biophysical characterization. Protein Expression and Purification, 2017, 134, 47-62.	0.6	5
49	Pathogenic implications of distinct patterns of iron and zinc in chronic MS lesions. Acta Neuropathologica, 2017, 134, 45-64.	3.9	94
50	Selenium-mediated arsenic excretion in mammals: a synchrotron-based study of whole-body distribution and tissue-specific chemistry. Metallomics, 2017, 9, 1585-1595.	1.0	34
51	Biological iron-sulfur storage in a thioferrate-protein nanoparticle. Nature Communications, 2017, 8, 16110.	5.8	20
52	Photochemically Generated Thiyl Free Radicals Observed by X-ray Absorption Spectroscopy. Journal of the American Chemical Society, 2017, 139, 11519-11526.	6.6	23
53	X-ray Absorption Spectroscopy of Aliphatic Organic Sulfides. Journal of Physical Chemistry A, 2017, 121, 6256-6261.	1.1	11
54	Remarkable differences in the biochemical fate of Cd ²⁺ , Hg ²⁺ , CH ₃ Hg ⁺ and thimerosal in red blood cell lysate. Metallomics, 2017, 9, 1060-1072.	1.0	26

#	Article	IF	CITATIONS
55	A Multimodal Spectroscopic Imaging Method To Characterize the Metal and Macromolecular Content of Proteinaceous Aggregates ("Amyloid Plaquesâ€). Biochemistry, 2017, 56, 4107-4116.	1.2	55
56	Multi-modal spectroscopic imaging with synchrotron light to study mechanisms of brain disease. Proceedings of SPIE, 2017, , .	0.8	0
57	Effects of inorganic mercury on the olfactory pits of zebrafish larvae. Metallomics, 2016, 8, 514-517.	1.0	8
58	Chemical Sensitivity of the Sulfur K-Edge X-ray Absorption Spectra of Organic Disulfides. Journal of Physical Chemistry A, 2016, 120, 7279-7286.	1.1	13
59	Tuning the metabolism of the anticancer drug cisplatin with chemoprotective agents to improve its safety and efficacy. Metallomics, 2016, 8, 1170-1176.	1.0	27
60	Insights into the Nature of the Chemical Bonding in Thiophene-2-thiol from X-ray Absorption Spectroscopy. Journal of Physical Chemistry A, 2016, 120, 6929-6933.	1.1	11
61	Trifluoroselenomethionine: A New Unnatural Amino Acid. ChemBioChem, 2016, 17, 1738-1751.	1.3	27
62	Imaging Taurine in the Central Nervous System Using Chemically Specific X-ray Fluorescence Imaging at the Sulfur K-Edge. Analytical Chemistry, 2016, 88, 10916-10924.	3.2	19
63	Chemical basis for the detoxification of cisplatin-derived hydrolysis products by sodium thiosulfate. Journal of Inorganic Biochemistry, 2016, 162, 96-101.	1.5	14
64	Confocal xâ€ray Fluorescence Imaging Facilitates Highâ€Resolution Elemental Mapping in Fragile Archaeological Bone. Archaeometry, 2016, 58, 207-217.	0.6	19
65	Observation of the seleno bis-(S-glutathionyl) arsinium anion in rat bile. Journal of Inorganic Biochemistry, 2016, 158, 24-29.	1.5	17
66	Chemical Biology in the Embryo: <i>In Situ</i> Imaging of Sulfur Biochemistry in Normal and Proteoglycan-Deficient Cartilage Matrix. Biochemistry, 2016, 55, 2441-2451.	1.2	13
67	Distribution of selenium in zebrafish larvae after exposure to organic and inorganic selenium forms. Metallomics, 2016, 8, 305-312.	1.0	36
68	Multispecies Biofilms Transform Selenium Oxyanions into Elemental Selenium Particles: Studies Using Combined Synchrotron X-ray Fluorescence Imaging and Scanning Transmission X-ray Microscopy. Environmental Science & Technology, 2016, 50, 10343-10350.	4.6	24
69	Arsenic transfer and biotransformation in a fully characterized freshwater food web. Coordination Chemistry Reviews, 2016, 306, 558-565.	9.5	9
70	CHAPTER 4. X-Ray Absorption Spectroscopy of Molybdenum and Tungsten Enzymes. 2-Oxoglutarate-Dependent Oxygenases, 2016, , 121-167.	0.8	2
71	Novel bio-spectroscopic imaging reveals disturbed protein homeostasis and thiol redox with protein aggregation prior to hippocampal CA1 pyramidal neuron death induced by global brain ischemia in the rat. Free Radical Biology and Medicine, 2015, 89, 806-818.	1.3	24
72	In Situ Biospectroscopic Investigation of Rapid Ischemic and Postmortem Induced Biochemical Alterations in the Rat Brain. ACS Chemical Neuroscience, 2015, 6, 226-238.	1.7	41

#	Article	IF	CITATIONS
73	Application of a spoked channel array to confocal X-ray fluorescence imaging and X-ray absorption spectroscopy of medieval stained glass. Journal of Analytical Atomic Spectrometry, 2015, 30, 759-766.	1.6	13
74	Selenium Preferentially Accumulates in the Eye Lens Following Embryonic Exposure: A Confocal X-ray Fluorescence Imaging Study. Environmental Science & Technology, 2015, 49, 2255-2261.	4.6	35
75	d ¹ Oxosulfido-Mo(V) Compounds: First Isolation and Unambiguous Characterization of an Extended Series. Inorganic Chemistry, 2015, 54, 6386-6396.	1.9	11
76	Phenylthiourea alters toxicity of mercury compounds in zebrafish larvae. Journal of Inorganic Biochemistry, 2015, 151, 10-17.	1.5	18
77	Soft tissue measurement of arsenic and selenium in an animal model using portable X-ray fluorescence. Radiation Physics and Chemistry, 2015, 116, 241-247.	1.4	11
78	Interaction of mercury and selenium in the larval stage zebrafish vertebrate model. Metallomics, 2015, 7, 1247-1255.	1.0	34
79	Structural basis of enzymatic benzene ring reduction. Nature Chemical Biology, 2015, 11, 586-591.	3.9	52
80	Synchrotron X-ray fluorescence imaging evidence of biogenic mercury identified in a burial in colonial Antigua. Journal of Archaeological Science, 2015, 58, 26-30.	1.2	12
81	High Affinity Binding of Indium and Ruthenium Ions by Gastrins. PLoS ONE, 2015, 10, e0140126.	1.1	5
82	EVIDENCE FOR BIOGENIC COPPER (HEMOCYANIN) IN THE MIDDLE CAMBRIAN ARTHROPOD MARRELLA FROM THE BURGESS SHALE. Palaios, 2014, 29, 512-524.	0.6	16
83	Synchrotron X-ray absorption spectroscopy analysis of arsenic chemical speciation in human nail clippings. Environmental Chemistry, 2014, 11, 632.	0.7	9
84	Structural characterization of Cd2+ complexes in solution with DMSA and DMPS. Journal of Inorganic Biochemistry, 2014, 136, 99-106.	1.5	12
85	The solution structure of the copper clioquinol complex. Journal of Inorganic Biochemistry, 2014, 133, 50-56.	1.5	26
86	Molybdenum and tungsten oxygen transferases – structural and functional diversity within a common active site motif. Metallomics, 2014, 6, 15-24.	1.0	47
87	Combined EXAFS and DFT Structure Calculations Provide Structural Insights into the 1:1 Multiâ€Histidine Complexes of Cu ^{II} , Cu ^I , and Zn ^{II} with the Tandem Octarepeats of the Mammalian Prion Protein. Chemistry - A European Journal, 2014, 20, 9770-9783.	1.7	21
88	Proteomics of Desulfovibrio desulfuricans and X-ray absorption spectroscopy to investigate mercury methylation in the presence of selenium. Metallomics, 2014, 6, 465.	1.0	25
89	Long-Range Chemical Sensitivity in the Sulfur K-Edge X-ray Absorption Spectra of Substituted Thiophenes. Journal of Physical Chemistry A, 2014, 118, 7796-7802.	1.1	31
90	Elemental and Chemically Specific X-ray Fluorescence Imaging of Biological Systems. Chemical Reviews, 2014, 114, 8499-8541.	23.0	234

#	Article	IF	CITATIONS
91	Methylmercury Targets Photoreceptor Outer Segments. ACS Chemical Biology, 2013, 8, 2256-2263.	1.6	40
92	New Insights into Metal Interactions with the Prion Protein: EXAFS Analysis and Structure Calculations of Copper Binding to a Single Octarepeat from the Prion Protein. Journal of Physical Chemistry B, 2013, 117, 13822-13841.	1.2	21
93	X-ray Absorption Spectroscopy of a Quantitatively Mo(V) Dimethyl Sulfoxide Reductase Species. Inorganic Chemistry, 2013, 52, 2830-2837.	1.9	26
94	Subcellular Biochemical Investigation of Purkinje Neurons Using Synchrotron Radiation Fourier Transform Infrared Spectroscopic Imaging with a Focal Plane Array Detector. ACS Chemical Neuroscience, 2013, 4, 1071-1080.	1.7	35
95	Copper chaperone Atox1 interacts with the metal-binding domain of Wilson's disease protein in cisplatin detoxification. Biochemical Journal, 2013, 454, 147-156.	1.7	53
96	X-Ray Absorption Spectroscopy of Metals in Biology. , 2013, , 2762-2767.		1
97	Chemical Form Matters: Differential Accumulation of Mercury Following Inorganic and Organic Mercury Exposures in Zebrafish Larvae. ACS Chemical Biology, 2012, 7, 411-420.	1.6	83
98	X-ray Absorption Spectroscopy at the Sulfur K-Edge: A New Tool to Investigate the Biochemical Mechanisms of Neurodegeneration. ACS Chemical Neuroscience, 2012, 3, 178-185.	1.7	61
99	X-ray-induced photo-chemistry and X-ray absorptionÂspectroscopy of biological samples. Journal of Synchrotron Radiation, 2012, 19, 875-886.	1.0	141
100	X-ray absorption spectroscopy at a protein crystallography facility: the Canadian Light Source beamline 08B1-1. Journal of Synchrotron Radiation, 2012, 19, 887-891.	1.0	3
101	International Workshop on Improving Data Quality and Quantity for XAFS Experiments (Q2XAFS 2011). Journal of Synchrotron Radiation, 2012, 19, 849-850.	1.0	7
102	Metalloprotein active site structure determination: Synergy between X-ray absorption spectroscopy and X-ray crystallography. Journal of Inorganic Biochemistry, 2012, 115, 127-137.	1.5	74
103	Knocking Out ACR2 Does Not Affect Arsenic Redox Status in Arabidopsis thaliana: Implications for As Detoxification and Accumulation in Plants. PLoS ONE, 2012, 7, e42408.	1.1	34
104	The fictile coordination chemistry of cuprous-thiolate sites in copper chaperones. Biochimica Et Biophysica Acta - Bioenergetics, 2012, 1817, 938-947.	0.5	27
105	The chemical forms of mercury and selenium in whale skeletal muscle. Metallomics, 2011, 3, 1232.	1.0	25
106	Prion protein expression level alters regional copper, iron and zinc content in the mouse brain. Metallomics, 2011, 3, 206.	1.0	91
107	Molybdenum Speciation in Uranium Mine Tailings Using X-Ray Absorption Spectroscopy. Environmental Science & Technology, 2011, 45, 455-460.	4.6	47
108	Molybdenum Site Structure of <i>Escherichia coli</i> YedY, a Novel Bacterial Oxidoreductase. Inorganic Chemistry, 2011, 50, 732-740.	1.9	21

#	Article	IF	CITATIONS
109	Nature of Halide Binding to the Molybdenum Site of Sulfite Oxidase. Inorganic Chemistry, 2011, 50, 9406-9413.	1.9	8
110	Towards a custom chelator for mercury: evaluation of coordination environments by molecular modeling. Journal of Biological Inorganic Chemistry, 2011, 16, 15-24.	1.1	16
111	Use of Soller slits to remove reference foil fluorescence from transmission spectra. Journal of Synchrotron Radiation, 2011, 18, 527-529.	1.0	5
112	Spectroscopic studies of molybdenum and tungsten enzymes. Coordination Chemistry Reviews, 2011, 255, 1055-1084.	9.5	74
113	Probing the coordination behavior of Hg2+, CH3Hg+, and Cd2+ towards mixtures of two biological thiols by HPLC-ICP-AES. Journal of Inorganic Biochemistry, 2011, 105, 375-381.	1.5	39
114	The chemical forms of mercury in human hair: a study using X-ray absorption spectroscopy. Journal of Biological Inorganic Chemistry, 2010, 15, 709-715.	1.1	30
115	Dynamic accumulation and redistribution of methylmercury in the lens of developing zebrafish embryos and larvae. Journal of Biological Inorganic Chemistry, 2010, 15, 1137-1145.	1.1	30
116	The Chemical Nature of Mercury in Human Brain Following Poisoning or Environmental Exposure. ACS Chemical Neuroscience, 2010, 1, 810-818.	1.7	168
117	The Structures of the C185S and C185A Mutants of Sulfite Oxidase Reveal Rearrangement of the Active Site. Biochemistry, 2010, 49, 3989-4000.	1.2	26
118	Active-Site Dynamics and Large-Scale Domain Motions of Sulfite Oxidase: A Molecular Dynamics Study. Journal of Physical Chemistry B, 2010, 114, 3266-3275.	1.2	25
119	Mapping metals in Parkinson's and normal brain using rapid-scanning x-ray fluorescence. Physics in Medicine and Biology, 2009, 54, 651-663.	1.6	112
120	Arsenic Kâ€edge Xâ€ray absorption spectroscopy of arsenic in seafood. Molecular Nutrition and Food Research, 2009, 53, 552-557.	1.5	14
121	Characterization of a modified nitrogenase Fe protein from Klebsiella pneumoniae in which the 4Fe4S cluster has been replaced by a 4Fe4Se cluster. Journal of Biological Inorganic Chemistry, 2009, 14, 673-682.	1.1	25
122	Molybdenum X-ray absorption edges from 200 to 20,000eV: The benefits of soft X-ray spectroscopy for chemical speciation. Journal of Inorganic Biochemistry, 2009, 103, 157-167.	1.5	40
123	Molybdenum Induces the Expression of a Protein Containing a New Heterometallic Mo-Fe Cluster in <i>Desulfovibrio alaskensis</i> . Biochemistry, 2009, 48, 873-882.	1.2	25
124	Unnatural Amino Acid Substitution as a Probe of the Allosteric Coupling Pathway in a Mycobacterial Cu(I) Sensor. Journal of the American Chemical Society, 2009, 131, 18044-18045.	6.6	54
125	Localizing the Chemical Forms of Sulfur in Vivo Using X-ray Fluorescence Spectroscopic Imaging: Application to Onion (<i>Allium cepa</i>) Tissues. Biochemistry, 2009, 48, 6846-6853.	1.2	43
126	Tracing Copperâ^'Thiomolybdate Complexes in a Prospective Treatment for Wilson's Disease. Biochemistry, 2009, 48, 891-897.	1.2	70

#	Article	IF	CITATIONS
127	Mechanisms of gold biomineralization in the bacterium <i>Cupriavidus metallidurans</i> . Proceedings of the United States of America, 2009, 106, 17757-17762.	3.3	283
128	The Chemical Forms of Mercury in Aged and Fresh Dental Amalgam Surfaces. Chemical Research in Toxicology, 2009, 22, 1761-1764.	1.7	19
129	Insect excretes unusual six-coordinate pentavalent arsenic species. Environmental Chemistry, 2009, 6, 298.	0.7	8
130	A possible molecular link between the toxicological effects of arsenic, selenium and methylmercury: methylmercury(II) seleno bis(S-glutathionyl) arsenic(III). Journal of Biological Inorganic Chemistry, 2008, 13, 461-470.	1.1	30
131	A new type of metal-binding site in cobalt- and zinc-containing adenylate kinases isolated from sulfate-reducers Desulfovibrio gigas and Desulfovibrio desulfuricans ATCC 27774. Journal of Inorganic Biochemistry, 2008, 102, 1380-1395.	1.5	16
132	Xâ€Ray Absorption Spectroscopy of Cuprousâ€Thiolate Clusters in <i>Saccharomyces cerevisiae</i> Metallothionein. Chemistry and Biodiversity, 2008, 5, 2042-2049.	1.0	19
133	Structure of the Molybdenum Site of Escherichia coli Trimethylamine N-Oxide Reductase. Inorganic Chemistry, 2008, 47, 1074-1078.	1.9	33
134	Mo ^V Electron Paramagnetic Resonance of Sulfite Oxidase Revisited: The Low-pH Chloride Signal. Inorganic Chemistry, 2008, 47, 2033-2038.	1.9	28
135	Electronic Structure Description of thecis-MoOS Unit in Models for Molybdenum Hydroxylases. Journal of the American Chemical Society, 2008, 130, 55-65.	6.6	58
136	A High-Affinity Metal-Binding Peptide from <i>Escherichia coli</i> HypB. Journal of the American Chemical Society, 2008, 130, 14056-14057.	6.6	37
137	Structural and Biological Analysis of the Metal Sites of <i>Escherichia coli</i> Hydrogenase Accessory Protein HypB. Biochemistry, 2008, 47, 11981-11991.	1.2	45
138	Chemical Forms of Mercury and Selenium in Fish Following Digestion with Simulated Gastric Fluid. Chemical Research in Toxicology, 2008, 21, 2106-2110.	1.7	47
139	Localizing organomercury uptake and accumulation in zebrafish larvae at the tissue and cellular level. Proceedings of the National Academy of Sciences of the United States of America, 2008, 105, 12108-12112.	3.3	129
140	X-Ray Absorption Spectroscopy as a Probe of Microbial Sulfur Biochemistry: the Nature of Bacterial Sulfur Globules Revisited. Journal of Bacteriology, 2008, 190, 6376-6383.	1.0	53
141	Chapter 5 Inorganic Molecular Toxicology and Chelation Therapy of Heavy Metals and Metalloids. Advances in Molecular Toxicology, 2008, 2, 123-152.	0.4	9
142	Copper sensing function of Drosophila metal-responsive transcription factor-1 is mediated by a tetranuclear Cu(I) cluster. Nucleic Acids Research, 2008, 36, 3128-3138.	6.5	40
143	Insights into the Chemical Biology of Selenium. Phosphorus, Sulfur and Silicon and the Related Elements, 2008, 183, 924-930.	0.8	8
144	Development of a combined K-edge subtraction and fluorescence subtraction imaging system for small animals. Review of Scientific Instruments, 2008, 79, 085102.	0.6	5

#	Article	IF	CITATIONS
145	The Characterization and Role of Zinc Binding in Yeast Cox4. Journal of Biological Chemistry, 2007, 282, 8926-8934.	1.6	35
146	Characterization of the Cytochrome c Oxidase Assembly Factor Cox19 of Saccharomyces cerevisiae. Journal of Biological Chemistry, 2007, 282, 10233-10242.	1.6	55
147	X-Ray Absorption Spectroscopy Imaging of Biological Tissues. AIP Conference Proceedings, 2007, , .	0.3	6
148	Mercury Speciation in Piscivorous Fish from Mining-Impacted Reservoirs. Environmental Science & Technology, 2007, 41, 2745-2749.	4.6	69
149	Interaction of Product Analogues with the Active Site ofRhodobacterSphaeroidesDimethyl Sulfoxide Reductase. Inorganic Chemistry, 2007, 46, 3097-3104.	1.9	21
150	Sulfur X-ray Absorption Spectroscopy of Living Mammalian Cells:  An Enabling Tool for Sulfur Metabolomics. In Situ Observation of Uptake of Taurine into MDCK Cells. Biochemistry, 2007, 46, 14735-14741.	1.2	24
151	Modified Active Site Coordination in a Clinical Mutant of Sulfite Oxidase. Journal of the American Chemical Society, 2007, 129, 9421-9428.	6.6	30
152	Synthesis, Characterization, and Biomimetic Chemistry of cis-Oxosulfidomolybdenum(VI) Complexes Stabilized by an Intramolecular Mo(O)S··ŶS Interaction. Inorganic Chemistry, 2007, 46, 939-948.	1.9	29
153	X-ray Absorption Spectroscopic Characterization of the Molybdenum Site ofEscherichia coliDimethyl Sulfoxide Reductase. Inorganic Chemistry, 2007, 46, 2-4.	1.9	24
154	Chemical Form of Selenium in Naturally Selenium-Rich Lentils (Lens culinarisL.) from Saskatchewan. Journal of Agricultural and Food Chemistry, 2007, 55, 7337-7341.	2.4	64
155	Reversed-phase high-performance liquid chromatographic separation of inorganic mercury and methylmercury driven by their different coordination chemistry towards thiols. Journal of Chromatography A, 2007, 1156, 331-339.	1.8	37
156	Strong poison revisited. Journal of Inorganic Biochemistry, 2007, 101, 1891-1893.	1.5	22
157	CsoR is a novel Mycobacterium tuberculosis copper-sensing transcriptional regulator. , 2007, 3, 60-68.		291
158	The chemical form of mitochondrial iron in Friedreich's ataxia. Journal of Inorganic Biochemistry, 2007, 101, 957-966.	1.5	36
159	X-RAY ABSORPTION SPECTROSCOPY IN BIOLOGY AND CHEMISTRY. , 2007, , 97-119.		14
160	Models for the Molybdenum Hydroxylases:Â Synthesis, Characterization and Reactivity ofcis-Oxosulfido-Mo(VI) Complexes. Journal of the American Chemical Society, 2006, 128, 305-316.	6.6	57
161	More on Molecular Mimicry in Mercury Toxicology. Chemical Research in Toxicology, 2006, 19, 1118-1120.	1.7	8
162	Localizing the Biochemical Transformations of Arsenate in a Hyperaccumulating Fern. Environmental Science & Technology, 2006, 40, 5010-5014.	4.6	195

#	Article	IF	CITATIONS
163	The Seleno Bis(S-glutathionyl) Arsinium Ion Is Assembled in Erythrocyte Lysate. Chemical Research in Toxicology, 2006, 19, 601-607.	1.7	62
164	Structure of the Active Site of Sulfite Dehydrogenase from Starkeya novella. Inorganic Chemistry, 2006, 45, 7488-7492.	1.9	24
165	Molecular Mimicry in Mercury Toxicology. Chemical Research in Toxicology, 2006, 19, 753-759.	1.7	71
166	High-Resolution EXAFS of the Active Site of Human Sulfite Oxidase:Â Comparison with Density Functional Theory and X-ray Crystallographic Results. Inorganic Chemistry, 2006, 45, 493-495.	1.9	38
167	A cadmium enzyme from a marine diatom. Nature, 2005, 435, 42-42.	13.7	518
168	High-Resolution X-Ray Emission Spectroscopy of Molybdenum Compounds ChemInform, 2005, 36, no.	0.1	0
169	Using softer X-ray absorption spectroscopy to probe biological systems. Journal of Synchrotron Radiation, 2005, 12, 392-401.	1.0	31
170	Human Sco1 and Sco2 Function as Copper-binding Proteins. Journal of Biological Chemistry, 2005, 280, 34113-34122.	1.6	147
171	High-Resolution X-ray Emission Spectroscopy of Molybdenum Compounds. Inorganic Chemistry, 2005, 44, 2579-2581.	1.9	22
172	Nature of the Catalytically Labile Oxygen at the Active Site of Xanthine Oxidase. Journal of the American Chemical Society, 2005, 127, 4518-4522.	6.6	86
173	X-ray Absorption Spectroscopy of Selenate Reductase. Inorganic Chemistry, 2004, 43, 402-404.	1.9	35
174	The Sulfur Chemistry of Shiitake Mushroom. Journal of the American Chemical Society, 2004, 126, 458-459.	6.6	42
175	Selenium Biotransformations in an Insect Ecosystem:Â Effects of Insects on Phytoremediation. Environmental Science & Technology, 2004, 38, 3581-3586.	4.6	59
176	C-Terminal Domain of the Membrane Copper Transporter Ctr1 from Saccharomyces cerevisiae Binds Four Cu(I) lons as a Cuprous-Thiolate Polynuclear Cluster:  Sub-femtomolar Cu(I) Affinity of Three Proteins Involved in Copper Trafficking. Journal of the American Chemical Society, 2004, 126, 3081-3090.	6.6	237
177	Coordination Chemistry at the Molybdenum Site of Sulfite Oxidase: Redox-Induced Structural Changes in the Cysteine 207 to Serine Mutant. Inorganic Chemistry, 2004, 43, 8456-8460.	1.9	31
178	Mercury Binding to the Chelation Therapy Agents DMSA and DMPS and the Rational Design of Custom Chelators for Mercury. Chemical Research in Toxicology, 2004, 17, 999-1006.	1.7	102
179	The Chemical Form of Mercury in Fish. Science, 2003, 301, 1203-1203.	6.0	1,214
180	Thioredoxinh overexpressed in barley seeds enhances selenite resistance and uptake during germination and early seedling development. Planta, 2003, 218, 186-191.	1.6	25

#	Article	IF	CITATIONS
181	Imaging of selenium in plants using tapered metal monocapillary optics. Journal of Synchrotron Radiation, 2003, 10, 289-290.	1.0	19
182	Structure of Frataxin Iron Cores: An X-ray Absorption Spectroscopic Studyâ€. Biochemistry, 2003, 42, 5971-5976.	1.2	68
183	Tetrathiomolybdate Causes Formation of Hepatic Copperâ^Molybdenum Clusters in an Animal Model of Wilson's Disease. Journal of the American Chemical Society, 2003, 125, 1704-1705.	6.6	59
184	Redox Interplay of Oxoâ^'Thioâ^'Tungsten Centers with Sulfur-Donor Co-Ligands. Inorganic Chemistry, 2003, 42, 5909-5916.	1.9	17
185	Chemical Form and Distribution of Selenium and Sulfur in the Selenium Hyperaccumulator Astragalus bisulcatus Â. Plant Physiology, 2003, 131, 1460-1467.	2.3	163
186	Recombinant Rhodobacter capsulatus Xanthine Dehydrogenase, a Useful Model System for the Characterization of Protein Variants Leading to Xanthinuria I in Humans. Journal of Biological Chemistry, 2003, 278, 20802-20811.	1.6	57
187	Yeast Cox11, a Protein Essential for Cytochrome cOxidase Assembly, Is a Cu(I)-binding Protein. Journal of Biological Chemistry, 2002, 277, 31237-31242.	1.6	143
188	Biliary Excretion of [(GS)2AsSe]-after Intravenous Injection of Rabbits with Arsenite and Selenate. Chemical Research in Toxicology, 2002, 15, 1466-1471.	1.7	76
189	The Active Site of Arsenite Oxidase from Alcaligenes faecalis. Journal of the American Chemical Society, 2002, 124, 11276-11277.	6.6	74
190	Unraveling the Substrateâ^'Metal Binding Site of Ferrochelatase:  An X-ray Absorption Spectroscopic Study. Biochemistry, 2002, 41, 4809-4818.	1.2	47
191	Structures of the Cuprous-Thiolate Clusters of the Mac1 and Ace1 Transcriptional Activators. Biochemistry, 2002, 41, 6469-6476.	1.2	81
192	Synthesis, Purification, and Structural Characterization of the Dimethyldiselenoarsinate Anion. Inorganic Chemistry, 2002, 41, 5426-5432.	1.9	27
193	Copper Transfer from the Cu(I) Chaperone, CopZ, to the Repressor, Zn(II)CopY:Â Metal Coordination Environments and Protein Interactionsâ€. Biochemistry, 2002, 41, 5822-5829.	1.2	116
194	Spectroscopic Studies of Pyrococcus furiosus Superoxide Reductase:  Implications for Active-Site Structures and the Catalytic Mechanism. Journal of the American Chemical Society, 2002, 124, 788-805.	6.6	120
195	Anthocyanins facilitate tungsten accumulation in Brassica. Physiologia Plantarum, 2002, 116, 351-358.	2.6	75
196	Solution structural studies of molybdate–nucleotide polyanions. Journal of Inorganic Biochemistry, 2002, 88, 274-283.	1.5	11
197	Synthesis, X-ray absorption spectroscopy and purification of the seleno-bis (S-glutathionyl) arsinium anion from selenide, arsenite and glutathione. Journal of Organometallic Chemistry, 2002, 650, 108-113.	0.8	20
198	Removal of a cysteine ligand from rubredoxin: assembly of Fe2S2 and Fe(S-Cys)3(OH) centres. Journal of Biological Inorganic Chemistry, 2002, 7, 781-790.	1.1	19

#	Article	IF	CITATIONS
199	X-ray absorption spectroscopy of bacterial sulfur globules. Microbiology (United Kingdom), 2002, 148, 2267-2268.	0.7	11
200	In situ observation of the generation of isothiocyanates from sinigrin in horseradish and wasabi. Biochimica Et Biophysica Acta - General Subjects, 2001, 1527, 156-160.	1.1	33
201	Fluorine Encapsulation and Stabilization of Biologically Relevant Low-Valence Copper-Oxo Cores. Inorganic Chemistry, 2001, 40, 4812-4813.	1.9	47
202	Analysis of Sulfur Biochemistry of Sulfur Bacteria Using X-ray Absorption Spectroscopy. Biochemistry, 2001, 40, 8138-8145.	1.2	153
203	Synthesis, Characterization, and Electrochemistry of cis-Oxothio- and cis-Bis(thio)tungsten(VI) Complexes of Hydrotris(3,5-dimethylpyrazol-1-yl)borate. Inorganic Chemistry, 2001, 40, 4563-4573.	1.9	29
204	The Mitochondrial Copper Metallochaperone Cox17 Exists as an Oligomeric, Polycopper Complexâ€. Biochemistry, 2001, 40, 743-751.	1.2	115
205	Human Cytosolic Iron Regulatory Protein 1 Contains a Linear Ironâ^'Sulfur Cluster. Journal of the American Chemical Society, 2001, 123, 10121-10122.	6.6	23
206	Yeast Sco1, a Protein Essential for Cytochrome cOxidase Function Is a Cu(I)-binding Protein. Journal of Biological Chemistry, 2001, 276, 42520-42526.	1.6	161
207	Molybdenum Sequestration in BrassicaSpecies. A Role for Anthocyanins?. Plant Physiology, 2001, 126, 1391-1402.	2.3	162
208	Deep Desulfurization of Extensively Hydrodesulfurized Middle Distillate Oil by Rhodococcus sp. Strain ECRD-1. Applied and Environmental Microbiology, 2001, 67, 1949-1952.	1.4	72
209	XAS and microscopy studies of the uptake and bio-transformation of copper in Larrea tridentata (creosote bush). Microchemical Journal, 2000, 65, 227-236.	2.3	53
210	Quantitative, chemically specific imaging of selenium transformation in plants. Proceedings of the National Academy of Sciences of the United States of America, 2000, 97, 10717-10722.	3.3	168
211	Reduction and Coordination of Arsenic in Indian Mustard. Plant Physiology, 2000, 122, 1171-1178.	2.3	525
212	Fate of Selenate and Selenite Metabolized by Rhodobacter sphaeroides. Applied and Environmental Microbiology, 2000, 66, 4849-4853.	1.4	74
213	Stoichiometry of Complex Formation between Copper(I) and the N-Terminal Domain of the Menkes Proteinâ€. Biochemistry, 2000, 39, 6857-6863.	1.2	49
214	A Novel Protein-Bound Copperâ^'Molybdenum Cluster. Journal of the American Chemical Society, 2000, 122, 8321-8322.	6.6	90
215	A Metabolic Link between Arsenite and Selenite:Â The Seleno-bis(S-glutathionyl) Arsinium Ion. Journal of the American Chemical Society, 2000, 122, 4637-4639.	6.6	132
216	Toward a Total Model for the Molybdenum Hydroxylases:Â Synthesis, Redox, and Biomimetic Chemistry of Oxo-thio-Mo(VI) and -Mo(V) Complexes. Journal of the American Chemical Society, 2000, 122, 2946-2947.	6.6	44

#	Article	IF	CITATIONS
217	Structural Basis of the Antagonism between Inorganic Mercury and Selenium in Mammals. Chemical Research in Toxicology, 2000, 13, 1135-1142.	1.7	158
218	The Active Site Structure of Thalassiosira weissflogii Carbonic Anhydrase 1. Biochemistry, 2000, 39, 12128-12130.	1.2	117
219	Structure of the Molybdenum Site of Rhodobacter sphaeroides Biotin Sulfoxide Reductase. Biochemistry, 2000, 39, 4046-4052.	1.2	33
220	Microbial Desulfurization of a Crude Oil Middle-Distillate Fraction: Analysis of the Extent of Sulfur Removal and the Effect of Removal on Remaining Sulfur. Applied and Environmental Microbiology, 1999, 65, 181-188.	1.4	96
221	Generation and biomimetic chemistry of tungsten–dithiolene complexes containing the hydrotris(3,5-dimethylpyrazol-1-yl)borate ligand. Journal of Inorganic Biochemistry, 1999, 76, 39-45.	1.5	15
222	X-ray absorption spectroscopy of selenium-containing amino acids. Journal of Biological Inorganic Chemistry, 1999, 4, 791-794.	1.1	66
223	X-ray absorption spectroscopy of cadmium phytochelatin and model systems. BBA - Proteins and Proteomics, 1999, 1429, 351-364.	2.1	83
224	Structure of the Molybdenum Site of Dimethyl Sulfoxide Reductase. Journal of the American Chemical Society, 1999, 121, 1256-1266.	6.6	149
225	Structural Changes Induced by Catalytic Turnover at the Molybdenum Site of Arabidopsis Nitrate Reductase. Journal of the American Chemical Society, 1999, 121, 9730-9731.	6.6	39
226	Observation of Ligand-Based Redox Chemistry at the Active Site of a Molybdenum Enzyme. Journal of the American Chemical Society, 1999, 121, 2625-2626.	6.6	52
227	X-ray Absorption Spectroscopy of Chicken Sulfite Oxidase Crystals. Inorganic Chemistry, 1999, 38, 2539-2540.	1.9	63
228	Microbial Desulfurization of a Crude Oil Middle-Distillate Fraction: Analysis of the Extent of Sulfur Removal and the Effect of Removal on Remaining Sulfur. Applied and Environmental Microbiology, 1999, 65, 3264-3264.	1.4	8
229	An edge with XAS. Nature Structural Biology, 1998, 5, 645-647.	9.7	41
230	Sulfur K-edge X-ray absorption spectroscopy for determining the chemical speciation of sulfur in biological systems. FEBS Letters, 1998, 441, 11-14.	1.3	150
231	The Rubredoxin fromClostridium pasteurianum:Â Mutation of the Iron Cysteinyl Ligands to Serine. Crystal and Molecular Structures of Oxidized and Dithionite-Treated Forms of the Cys42Ser Mutant. Journal of the American Chemical Society, 1998, 120, 4135-4150.	6.6	81
232	X-ray Absorption Spectroscopy of the Molybdenum Site ofEscherichia coliFormate Dehydrogenase. Journal of the American Chemical Society, 1998, 120, 1267-1273.	6.6	90
233	Characterization of the Copper Chaperone Cox17 ofSaccharomyces cerevisiaeâ€. Biochemistry, 1998, 37, 7572-7577.	1.2	111
234	ATP Sulfurylases from Sulfate-Reducing Bacteria of the GenusDesulfovibrio.A Novel Metalloprotein Containing Cobalt and Zincâ€. Biochemistry, 1998, 37, 16225-16232.	1.2	76

#	Article	IF	CITATIONS
235	Interaction of Arsenate with the Molybdenum Site of Sulfite Oxidase. Journal of the American Chemical Society, 1998, 120, 4522-4523.	6.6	38
236	Oxotungsten(VI) Chemistry of Hydrotris(3,5-dimethylpyrazol-1-yl)borate:Â Hydroxodioxotungsten(VI), Trioxotungsten(VI), and (μ-Oxo)bis[dioxotungsten(VI)] Complexes. Inorganic Chemistry, 1997, 36, 472-479.	1.9	22
237	The remarkable complexity of hydroxylamine oxidoreductase. Nature Structural Biology, 1997, 4, 247-250.	9.7	19
238	X-ray absorption spectroscopy of molybdenum enzymes. Journal of Biological Inorganic Chemistry, 1997, 2, 790-796.	1.1	30
239	Presence of a Copper(I)â^'Thiolate Regulatory Domain in the Copper-Activated Transcription Factor Amt1â€. Biochemistry, 1996, 35, 14583-14589.	1.2	53
240	Electron Paramagnetic Resonance Spectroscopy of the Ironâ^'Molybdenum Cofactor ofClostridium pasteurianumNitrogenase. Inorganic Chemistry, 1996, 35, 434-438.	1.9	23
241	X-ray Absorption Spectroscopy of Dimethyl Sulfoxide Reductase fromRhodobacter sphaeroides. Journal of the American Chemical Society, 1996, 118, 1113-1117.	6.6	123
242	Dinitrogen Cleavage by Three-Coordinate Molybdenum(III) Complexes:Â Mechanistic and Structural Data1. Journal of the American Chemical Society, 1996, 118, 8623-8638.	6.6	394
243	X-ray absorption spectroscopy of Pyrococcus furiosus rubredoxin. Journal of Biological Inorganic Chemistry, 1996, 1, 226-230.	1.1	20
244	The Molybdenum Site of Sulfite Oxidase:Â A Comparison of Wild-Type and the Cysteine 207 to Serine Mutant Using X-ray Absorption Spectroscopy. Journal of the American Chemical Society, 1996, 118, 8588-8592.	6.6	123
245	Cytochrome f revealed. Trends in Biochemical Sciences, 1995, 20, 217-218.	3.7	20
246	Alteration of Axial Coordination by Protein Engineering in Myoglobin. Journal of Biological Chemistry, 1995, 270, 15993-16001.	1.6	63
247	Polarized X-ray Absorption Spectroscopy of Cupric Chloride Dihydrate. Inorganic Chemistry, 1995, 34, 3142-3152.	1.9	82
248	Mixed Cu+ and Zn2+ Coordination in the DNA-Binding Domain of the AMT1 Transcription Factor from Candida glabrata. Biochemistry, 1994, 33, 9566-9577.	1.2	55
249	Diffraction anomalous fine structure: a new technique for probing local atomic environment. Journal of the American Chemical Society, 1993, 115, 6302-6311.	6.6	73
250	X-ray absorption spectroscopy of oriented cytochrome oxidase. Biochimica Et Biophysica Acta - Bioenergetics, 1993, 1142, 240-252.	0.5	35
251	X-ray absorption spectroscopy of light elements in biological systems. Current Opinion in Structural Biology, 1993, 3, 780-784.	2.6	16
252	Nickel K-edge x-ray absorption fine structure of lithium nickel oxides. Journal of the American Chemical Society, 1993, 115, 4137-4144.	6.6	72

15

#	Article	IF	CITATIONS
253	Direct observation of bis-sulfur ligation to the heme of bacterioferritin. Journal of the American Chemical Society, 1993, 115, 7716-7718.	6.6	30
254	X-ray absorption spectroscopy of cuprous-thiolate clusters in proteins and model systems. Journal of the American Chemical Society, 1993, 115, 9498-9505.	6.6	148
255	Distinct metal binding configurations in ACE1. Biochemistry, 1993, 32, 7294-7301.	1.2	35
256	Site-Specific X-ray Absorption Spectroscopy Using DIFFRAXAFS. Japanese Journal of Applied Physics, 1993, 32, 206.	0.8	11
257	Cuprous-Thiolate Polymetalic Clusters in Biology. , 1993, , 110-123.		11
258	Aldehyde ferredoxin oxidoreductase from the hyperthermophilic archaebacterium Pyrococcus furiosus contains a tungsten oxo-thiolate center. Journal of the American Chemical Society, 1992, 114, 3521-3523.	6.6	69
259	Characterization and thermal reactivity of oxidized organic sulphur forms in coals. Fuel, 1992, 71, 1255-1264.	3.4	66
260	Coordination structure of the ferric heme iron in engineered distal histidine myoglobin mutants. Journal of Biological Chemistry, 1992, 267, 22843-52.	1.6	85
261	Surface composition of iron and inorganic sulfur forms in Argonne Premium coals by x-ray photoelectron spectroscopy. Energy & Fuels, 1991, 5, 720-723.	2.5	19
262	XANES evidence for selective organic sulfur removal from Illinois No. 6 coal. Energy & Fuels, 1991, 5, 771-773.	2.5	12
263	Direct determination and quantification of sulfur forms in coals from the Argonne Premium Sample Program. Energy & Fuels, 1991, 5, 93-97.	2.5	175
264	A copper-thiolate polynuclear cluster in the ACE1 transcription factor Proceedings of the National Academy of Sciences of the United States of America, 1991, 88, 6127-6131.	3.3	119
265	Thermal reactivity of sulphur forms in coal. Fuel, 1991, 70, 396-402.	3.4	67
266	Direct Determination and Quantification of Sulfur Forms in Heavy Petroleum and Coal. ACS Symposium Series, 1991, , 127-136.	0.5	5
267	COMPARISON OF PYROLYTIC AND X-RAY SPECTROSCOPIC METHODS FOR DETERMINING ORGANIC SULFUR SPECIES IN COAL. , 1991, , 985-988.		3
268	Direct determination and quantification of sulphur forms in heavy petroleum and coals. Fuel, 1990, 69, 945-949.	3.4	86
269	Chemistry of organically bound sulphur forms during the mild oxidation of coal. Fuel, 1990, 69, 1065-1067.	3.4	56
270	L-Edge spectroscopy of molybdenum compounds and enzymes. Journal of the American Chemical Society, 1990, 112, 2541-2548.	6.6	68

#	Article	IF	CITATIONS
271	Tryptophan radicals. Trends in Biochemical Sciences, 1990, 15, 170-172.	3.7	31
272	Sulfur K-Edge X-ray Absorption Spectroscopy of Petroleum Asphaltenes and Model Compounds. ACS Symposium Series, 1990, , 220-230.	0.5	4
273	The Manganese Cluster of the Water-Splitting Enzyme. , 1990, , 685-692.		2
274	Oriented x-ray absorption spectroscopy of membrane bound metalloproteins. Physica B: Condensed Matter, 1989, 158, 81-83.	1.3	13
275	Structure of the active site of sulfite oxidase. X-ray absorption spectroscopy of the molybdenum(IV), molybdenum(V), and molybdenum(VI) oxidation states. Biochemistry, 1989, 28, 5075-5080.	1.2	132
276	The manganese site of the photosynthetic water-splitting enzyme. Science, 1989, 243, 789-791.	6.0	210
277	Oxo-molybdenum(V) complexes with sulfide and hydrogensulfide ligands: models for the molybdenum(V) centers of xanthine oxidase and xanthine dehydrogenase. Inorganic Chemistry, 1989, 28, 8-10.	1.9	30
278	EXAFS analysis of xanthine oxidase complexes with alloxanthine, violapterin, and 6-pteridylaldehyde. Inorganic Chemistry, 1989, 28, 4018-4022.	1.9	74
279	Sulfur K-edge x-ray absorption spectroscopy of petroleum asphaltenes and model compounds. Journal of the American Chemical Society, 1989, 111, 3182-3186.	6.6	255
280	X-ray-absorption and electron-paramagnetic-resonance spectroscopic studies of the environment of molybdenum in high-pH and low-pH forms of Escherichia coli nitrate reductase. Biochemical Journal, 1989, 259, 693-700.	1.7	49
281	E.p.rspectroscopic studies on the molybdenum–iron site of nitrogenase from <i>Clostridium pasteurianum</i> . Biochemical Journal, 1989, 262, 349-352.	1.7	7
282	X-ray-absorption-spectroscopic evidence for a novel iron cluster in hydrogenase II from Clostridium pasteurianum. Biochemical Journal, 1989, 259, 597-600.	1.7	21
283	Spectroscopic properties of the hydroxylase of methane monooxygenase. BBA - Proteins and Proteomics, 1988, 952, 220-229.	2.1	44
284	Studies by electron paramagnetic resonance spectroscopy of xanthine oxidase enriched with molybdenum-97. Biochemistry, 1988, 27, 3603-3609.	1.2	87
285	X-ray crystallography and the spectroscopic imperative: The story of the [3Fe-4S] clusters. Trends in Biochemical Sciences, 1988, 13, 369-370.	3.7	19
286	The nature of the phosphate complex of sulphite oxidase from electron-paramagnetic-resonance studies. Biochemical Journal, 1988, 256, 307-309.	1.7	36
287	X-ray absorption studies of yeast copper metallothionein Journal of Biological Chemistry, 1988, 263, 8199-8203.	1.6	74
288	X-ray absorption studies of yeast copper metallothionein. Journal of Biological Chemistry, 1988, 263, 8199-203.	1.6	58

#	Article	IF	CITATIONS
289	Extended X-ray absorption fine structure studies of transient species during xanthine oxidase turnover by using rapid freezing. Biochemical Society Transactions, 1986, 14, 651-652.	1.6	24
290	X-ray absorption studies of the copper-beta domain of rat liver metallothionein. Journal of Inorganic Biochemistry, 1986, 27, 213-220.	1.5	40
291	Electron-paramagnetic-resonance studies using pre-steady-state kinetics and substitution with stable isotopes on the mechanism of action of molybdoenzymes. Biochemical Society Transactions, 1985, 13, 560-567.	1.6	84
292	Complexes with halide and other anions of the molybdenum centre of nitrate reductase from <i>Escherichia coli</i> . Biochemical Journal, 1985, 227, 925-931.	1.7	64
293	The proton spin-flip lines of Mo(V) EPR signals from sulfite oxidase and xanthine oxidase. Journal of Magnetic Resonance, 1985, 64, 384-394.	0.5	4
294	The structure of the inhibitory complex of alloxanthine (1H-pyrazolo[3,4-d]pyrimidine-4,6-diol) with the molybdenum centre of xanthine oxidase from electron-paramagnetic-resonance spectroscopy. Biochemical Journal, 1984, 218, 961-968.	1.7	63
295	Formamide as a substrate of xanthine oxidase. Biochemical Journal, 1984, 220, 235-242.	1.7	32
296	Electron-paramagnetic-resonance spectroscopy studies on the dissimilatory nitrate reductase from <i>Pseudomonas aeruginosad</i> . Biochemical Journal, 1984, 224, 601-608.	1.7	30
297	Formation of the inhibitory complex of p-mercuribenzoate with xanthine oxidase, evaluation of hyperfine and quadrupole couplings of mercury to molybdenum(V) from the electron paramagnetic resonance spectrum, and structure of the complex. Biochemistry, 1983, 22, 5443-5452.	1.2	20
298	Reaction of arsenite ions with the molybdenum center of milk xanthine oxidase. Biochemistry, 1983, 22, 1013-1021.	1.2	43
299	Studies by electron-paramagnetic-resonance spectroscopy of the molybdenum centre of aldehyde oxidase. Biochemical Journal, 1982, 203, 263-267.	1.7	23
300	Coupling of [33S]sulphur to molybdenum(V) in different reduced forms of xanthine oxidase. Biochemical Journal, 1981, 199, 629-637.	1.7	36